Structural Engineering and Mechanics, *Vol. 57, No. 4 (2016) 587-602*
DOI: http://dx.doi.org/10.12989/sem.2016.57.4.587

A response surface method based on sub-region of interest for structural reliability analysis

Weitao Zhao*, Xueyan Shi and Kai Tang

Key Laboratory of Liaoning Province for Composite Structural Analysis of Aerocraft and Simulation, Shenyang Aerospace University, Shenyang, 110-136, China

(Received May 20, 2015, Revised December 9, 2015, Accepted December 10, 2015)

Abstract. In structural reliability analysis, the response surface method is widely adopted because of its numerical efficiency. It should be understood that the response function must approximate the actual limit state function accurately in the main region influencing failure probability where it is evaluated. However, the size of main region influencing failure probability was not defined clearly in current response surface methods. In this study, the concept of sub-region of interest is constructed, and an improved response surface method is proposed based on the sub-region of interest. The sub-region of interest can clearly define the size of main region influencing failure probability, so that the accuracy of the evaluation of failure probability is increased. Some examples are introduced to demonstrate the efficiency and the accuracy of the proposed method for both numerical and implicit limit state functions.

Keywords: structural reliability; response surface; sub-region of interest; failure probability

1. Introduction

In structural reliability analysis, the calculation of failure probability is not easy in the absence of an explicit limit state function (LSF). Although Monte Carlo simulation (MCS) can give an exact solution, it is time-consuming for large and complex structures with low failure probabilities and implicit LSFs (Mohammadi *et al.* 2015). In order to reduce the number of finite element analyses, the first order reliability method (FORM) and the second order reliability method (SORM) were developed (Hasofer and Lind 1974, Ditlevsen and Madsen 1996, Kiureghian *et al.*1987). However, the accuracy of FORM is not enough for highly non-linear LSFs. Although SORM can improve the accuracy of the evaluation of failure probability, it involves complicated calculations to obtain Hessian matrix (Ditlevsen and Madsen 1996). In order to overcome the above problems, the response surface method (RSM) was proposed as a collection of statistical and mathematical techniques (Khuri and Cornell 1997, Myers and Montgomery 2008). In the RSM, the LSF is replaced by the response function (RF) of basic random variables. The RF is then used instead of the actual LSF for the estimation of failure probability. The RSM approximates the actual LSF by using experimental points and explicit mathematical functions (typically quadratic polynomials). As the RF is explicit, FORM or SORM can be applied to evaluate the failure

*Corresponding author, Associate Professor, E-mail: zhwt201@163.com

http://www.techno-press.org/?journal=sem&subpage=8 ISSN: 1225-4568 (Print), 1598-6217 (Online)

probability directly. Alternatively, MCS can be used efficiently since the evaluation of RF requires very little computational efforts.

Several researchers proposed improvements of the RSM in order to evaluate efficiently the failure probability of a complex structure. Bucher and Bourgund (1990) proposed a quadratic polynomial without cross terms. The RF represents the LSF along the coordinate axes of the space of standard normal random variables. Rajashekhar and Ellingwood (1993) proposed some ideas to improve the RF obtained from Bucher's algorithm, in which more iterations are repeated until the convergence parameter becomes very small or zero. Usually, the approach given by Rajashekhar and Ellingwood (1993) is called the classical RSM. Kim and Na (1997) proposed to arrange the experimental points in order to bring them close to the actual LSF by using the gradient projection technique. Gayton *et al*. (2003) proposed a RSM named CQ2RS (Complete Quadratic Response Surface with ReSampling). The method takes into account the knowledge of the engineer, and the statistical resampling technique is used to determine the design point. Wong *et al*. (2005) suggested to choose a $2n+1$ axial point design and to select a parameter f as a decreasing function of the coefficient of variation of random variables, where n is the number of random variables. Kaymaz and Chris (2005) proposed a new RSM called ADAPRES (a short form of adaptive response surface method), in which a weighted regression method is applied in place of the normal regression. Duprat and Sellier (2006) suggested that points efficiently positioned with respect to the design point are reused in the new iteration of the experimental design. Gavin and Yau (2008) presented the use of higher order polynomials function, the authors proposed to use a polynomial without a fixed degree in order to fit better the LSF under investigation. Nguyen *et al*. (2009) proposed an adaptive RSM based on a double weighted regression technique. For the first iteration, a linear RF is chosen, for the following iterations, a quadratic polynomials with cross terms is considered according to complementary points. Allaix and Carbone (2011) discussed the locations of the experimental points used to evaluate parameters of the RF. The locations of the experimental points are chosen according to the importance sensitivity of each random variable. At each iteration, a quadratic polynomials with cross terms is built after rotating the coordinate system. Basaga *et al*. (2012) proposed an improved RSM. In the algorithm, a quadratic approximate function is formed and the design point is determined with FORM, a point close to the LSF is searched using the design point, a vector projected method is used to generate sample points, and SORM is performed to obtain reliability index and probability of failure. Roussouly *et al*. (2013) proposed a new adaptive RSM, a RF is built from an initial Latin-Hyper cube Sampling (LHS) where the most significant terms are chosen from statistical criteria and cross-validation method. At each step, the LHS is refined in a region of interest defined with respect to an importance level on probability density in the design point. In order to find a good evaluation for the design point at the first iteration, Zhao and Qiu (2013) constructed the control point of experimental points. The new center point of experimental points is chosen by using the control point. The control point can guarantee that the center point of experimental points lies exactly on the failure surface and is close to the actual design point. Zhao *et al*. (2013) proposed an efficient RSM considering the nonlinear trend of the actual LSF, experimental points are selected close to the design point and can consider the nonlinear trend of the limit state. Linear, quadratic and cubic polynomials without cross terms are utilized to approximate the actual LSF. Su *et al*. (2015) proposed a Gaussian process (GP)-based response surface method, an iterative algorithm is proposed to improve the precision of GP approximation around the design point by constantly adding new design points to the initial training set.

As seen from above short literature review, since the region around design point gives the main

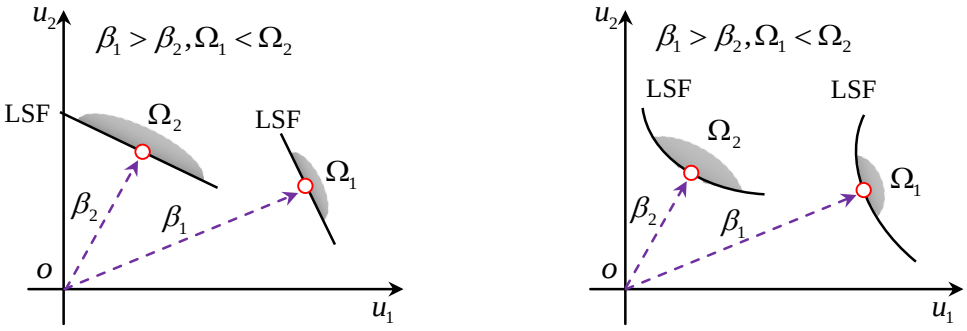

(a) Linear LSFs (b) Nonlinear LSFs

Fig. 1 Main regions in the two-dimensional standard normal space

contribution to failure probability (Ditlevsen and Madsen 1996), most improved RSMs focus on approximating the actual LSF at the region around design point. Despite their differences, main steps of procedures are always the same and can be summarized as follows:

1. Choose initial experimental points;
2. Build a RF;
3. Find the design point and the reliability index based on the RF;
4. Add new experimental points at the region around design point;
5. Repeat from the step 2 until a convergence criterion is satisfied.

However, the size of the region around design point was not given clearly in most improved RSMs, so that the size of main region influencing failure probability is ambiguous. In fact, the size of main region influencing failure probability for different LSFs is not the same. In general, the size of main region influencing failure probability is inversely proportional to the reliability index β. In the two-dimensional standard normal space (**U** space), the size of main region influencing failure probability is shown in Fig. 1. In Fig. 1, the shaded regions Ω_i (i=1, 2) represent the size of main regions influencing failure probability. Based on the structural reliability theory (Ditlevsen and Madsen 1996), if $\beta_1 > \beta_2$, then $\Omega_1 < \Omega_2$. It should be understood that the RF must approximate the actual LSF accurately in the main region influencing failure probability where it is evaluated. Thus, in order to accurately evaluate the failure probability using the RF, the main region influencing failure probability must be defined clearly.

In this work, in order to improve the accuracy of the evaluation of failure probability, the size of main region influencing failure probability is defined clearly. A different approach is proposed based on the size of main region. The proposed method can ensure that the fitting precision of the RF to the actual LSF in the main region is satisfied, so that the accuracy of the evaluation of failure probability is increased.

2. Definition of the sub-region of interest

In the paper, the size of main region influencing failure probability is defined, and the main region is called sub-region of interest. Based on the structural reliability theory (Ditlevsen and Madsen 1996), the main contribution to the failure probability comes from the region close to the design point.

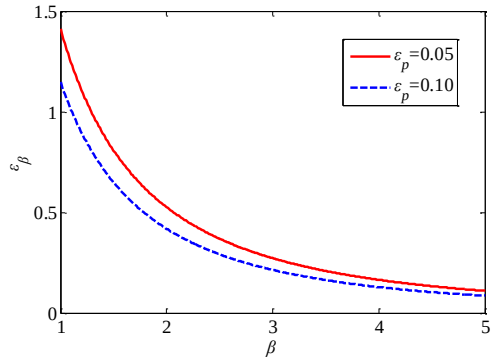

Fig. 2 Relationship between ε_β and β

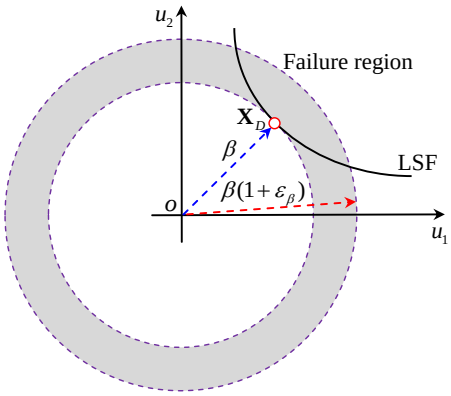

Fig. 3 Sub-region parameter in the two-dimensional standard normal space

2.1 Sub-region parameter

The relationship between failure probability and reliability index can be expressed as

$$P_f = \Phi(-\beta) \tag{1}$$

where P_f is the failure probability, β is the reliability index, and Φ is the standard normal cumulative distribution function.

For a given value of importance level ε_p, the sub-region parameter ε_β is defined by

$$\Phi[-\beta(1+\varepsilon_\beta)] = \varepsilon_p \Phi(-\beta) \tag{2}$$

We have

$$\varepsilon_\beta = -\frac{\Phi^{-1}[\varepsilon_p \Phi(-\beta)]}{\beta} - 1 \tag{3}$$

where Φ^{-1} is the standard normal inverse cumulative distribution function.

The relationship between ε_β and β is shown graphically in Fig. 2. As seen from Fig. 2, for a given value of importance level ε_p, ε_β is inversely proportional to β, namely if the reliability index is big then the size of main region influencing failure probability should be small; if the reliability index is small then the size of main region influencing failure probability should be big. This conclusion is to accord with the theory of structural reliability. In addition, as seen from Fig. 2, for a given value of β, ε_β decreases with increment of ε_p, namely the value of ε_β depends on the value of ε_p. In the paper, the different values of ε_p will be discussed in examples.

In the two-dimensional standard normal space, the sub-region parameter ε_β is shown in Fig. 3. In Fig. 3, $\mathbf{X}_D$ denotes the design point. Based on the concept of reliability index and Eq. (2), the contribution to failure probability coming from the sub-region, which is the region outside of β hypersphere and inside of $\beta(1+\varepsilon_\beta)$ hypersphere, should be 1-ε_p. For example, the reliability index β=3 and the failure probability $P_f=\Phi(-\beta)=\Phi(-3)=1.3499\times10^{-3}$. For a given value of importance level ε_p, such as 0.05, we obtain ε_β=0.2724. The failure probability $P_f^* = \Phi[-\beta(1+\varepsilon_\beta)] = 6.7495\times10^{-5}$, the ratio of $P_f^*/P_f = \varepsilon_p = 0.05$. The contribution to failure probability coming from the

sub-region (the shaded region in Fig. 3) is $(P_f - P_f^*)/P_f$ =1-ε_p=95%. Therefore, for a given value of importance level ε_p, sub-region parameter ε_β can define the size of main region influencing failure probability.

2.2 Size of the sub-region of interest

As seen from Fig. 3, the sub-region defined by ε_β is very big (the shaded region in Fig. 3), this sub-region contains the region away from the design point. However, the contribution to failure probability coming from the region away from the design point is very small. Thus, the sub-region defined by ε_β should be reduced. In the paper, two reference points $\mathbf{X}_{R1}$ and $\mathbf{X}_{R2}$ are constructed in the standard normal space, as follows

$$\mathbf{X}_{R1} = \mathbf{X}_D + \beta\varepsilon_\beta\boldsymbol{\omega} \tag{4}$$

$$\mathbf{X}_{R2} = \mathbf{X}_D - \beta\varepsilon_\beta\boldsymbol{\omega} \tag{5}$$

where $\mathbf{X}_D$ is the design point, $\boldsymbol{\omega}$ is the unit vector form the origin to $\mathbf{X}_D$.

Two hyperplanes using $\mathbf{X}_{R1}$, $\mathbf{X}_{R2}$ and $\boldsymbol{\omega}$ are constructed in the standard normal space, as follows

$$(\mathbf{X} - \mathbf{X}_{R1})^T\boldsymbol{\omega} = 0 \tag{6}$$

$$(\mathbf{X} - \mathbf{X}_{R2})^T\boldsymbol{\omega} = 0 \tag{7}$$

And then, a hypersphere is constructed in the standard normal space, its central point is $\mathbf{X}_D$ and its radius is R_D, as follows

$$(\mathbf{X} - \mathbf{X}_D)^T(\mathbf{X} - \mathbf{X}_D) - R_D^2 = 0 \tag{8}$$

The radius R_D is the distance from the design point to a special point in the standard normal space, the special point is a intersection point of the $\beta(1+\varepsilon_\beta)$ hypersphere and the tangent hyperplane through the design point. The value of R_D can be given by

$$R_D = \sqrt{[\beta(1+\varepsilon_\beta)]^2 - \beta^2} \tag{9}$$

In the two-dimensional standard normal space, the radius R_D is shown in Fig. 4.

The sub-region of interest in the standard normal space, say D_s, can be defined by using Eqs. (6), (7) and (8), as follows

$$D_s = D_1 \; n \; D_2 \; n \; D_3 \tag{10}$$

where D_1 represents the region of $(\mathbf{X}-\mathbf{X}_{R1})^T\boldsymbol{\omega}\geq 0$, D_2 represents the region of $(\mathbf{X}-\mathbf{X}_{R2})^T\boldsymbol{\omega}\leq 0$, and D_3 represents the region of $(\mathbf{X}-\mathbf{X}_D)^T(\mathbf{X}-\mathbf{X}_D)- R_D^2\leq 0$.

In the two-dimensional standard normal space, the sub-region of interest is shown in Fig. 5. As seen from Fig. 5, the sub-region of interest can contain the region around the design point defined by the sub-region parameter ε_β. Namely, the sub-region of interest can define the size of main region influencing failure probability.

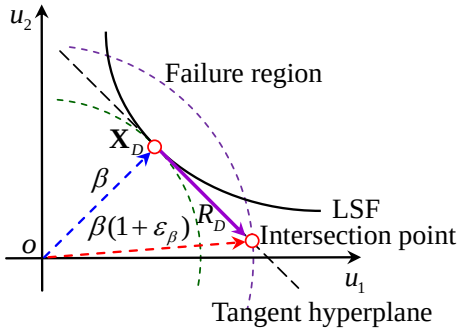

Fig. 4 The radius R_D in the two-dimensional standard normal space

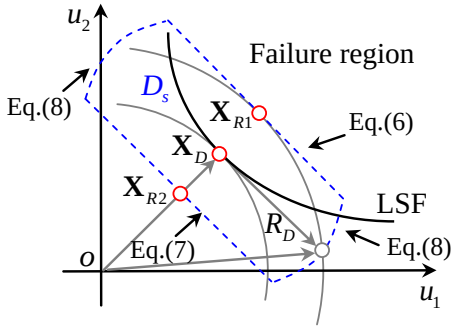

Fig. 5 The sub-region of interest in the two-dimensional standard normal space

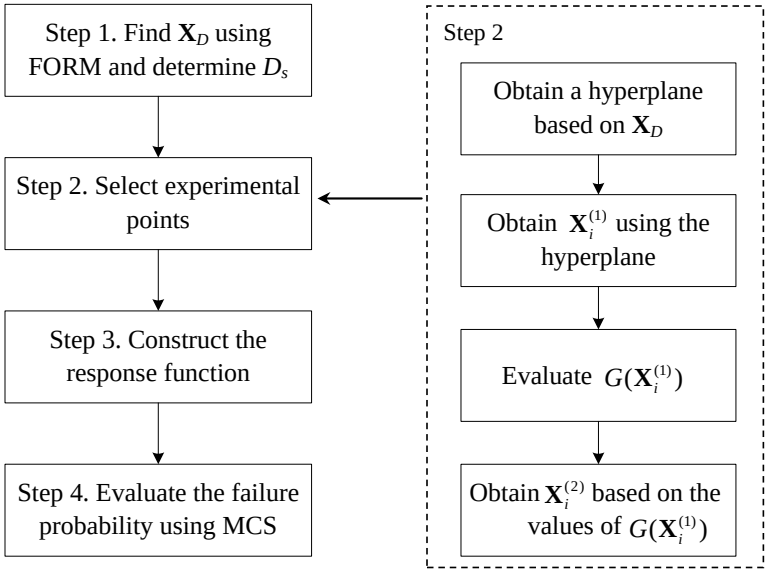

Fig. 6 The flowchart of the proposed RSM

3. An improved RSM

As seen from the above analysis of Section 2, for a given value of importance level ε_p, the sub-region of interest can be obtained when the design point is known. Usually, the design point is unknown before the sub-region of interest is constructed. However, the main purpose of the paper focuses on the sub-region of interest, and verifies that the sub-region of interest is reasonable and feasible. Thus, FORM is used to find the design point before the sub-region of interest is constructed in this paper.

The algorithm of the proposed method has four stages. Firstly, FORM (Hasofer and Lind 1974, Rackwitz-Fiessler 1978) is used to find the design point, and the size of sub-region of interest is defined; Secondly, experimental points considering the size of sub-region of interest are selected based on the design point; Thirdly, a RF (a quadratic polynomial function without cross terms) is used to approximate the actual LSF; Fourthly, the importance sampling MCS is utilized to evaluate

the failure probability by using the RF. A flowchart of the proposed method is shown in Fig. 6, and detailed steps are as follows:

3.1 Selection of experimental points

1. Find the design point $\mathbf{X}_D$ by using FORM, and define the size of sub-region of interest.

2. Obtain the tangent hyperplane through the design point $\mathbf{X}_D$ in the standard normal space. The expression of the tangent hyperplane is given by

$$(\mathbf{X}-\mathbf{X}_D)^T\boldsymbol{\omega}=0 \tag{11}$$

A intersection point of the tangent hyperplane and the ith coordinate axis is denoted by $\mathbf{X}_i^c$ (i=1,2,*L*,n), n is the number of random variables.

3. Select n experimental points along the direction form $\mathbf{X}_D$ to $\mathbf{X}_i^c$ in the standard normal space, as follows

$$\mathbf{X}_i^{(1)}=\mathbf{X}_D+R_D\boldsymbol{\gamma}_i \qquad i=1,2,...,n \tag{12}$$

where $\boldsymbol{\gamma}_i$ is the unit vector form the $\mathbf{X}_D$ to $\mathbf{X}_i^c$, and R_D is given by Eq. (9).

4. Evaluate the LSF $G(\mathbf{X}_i^{(1)})$ with respect to experimental points selected in sub-step 3.

5. Select n experimental points according to the values of $G(\mathbf{X}_i^{(1)})$ in the standard normal space, as follows

$$\mathbf{X}_i^{(2)}=\begin{cases}0.5(\mathbf{X}_D+\mathbf{X}_i^{(1)})+\dfrac{\beta\varepsilon_\beta}{2}\boldsymbol{\omega} & G(\mathbf{X}_i^{(1)})>0\\ 0.5(\mathbf{X}_D+\mathbf{X}_i^{(1)})-\dfrac{\beta\varepsilon_\beta}{2}\boldsymbol{\omega} & G(\mathbf{X}_i^{(1)})<0\\ 0.5(\mathbf{X}_D+\mathbf{X}_i^{(1)}) & G(\mathbf{X}_i^{(1)})=0\end{cases} \qquad i=1,2,...,n \tag{13}$$

As seen from Eqs. (12) and (13), the experimental points $\mathbf{X}_i^{(1)}$ lie on the boundary of sub-region of interest, the experimental points $\mathbf{X}_i^{(2)}$ can both consider the size of sub-region of interest and the design point. In the two-dimensional standard normal space, experimental points $\mathbf{X}_i^{(1)}$, $\mathbf{X}_i^{(2)}$ and the design point $\mathbf{X}_D$ are shown in Fig. 7.

3.2 Response function construction

The experimental points $\mathbf{X}_i^{(1)}$, $\mathbf{X}_i^{(2)}$ and the design point $\mathbf{X}_D$ are used to solve for the unknown coefficients of RF. Since these experimental points can consider the size of sub-region of interest and the design point, the fitting precision of the RF to the actual LSF in the sub-region of interest is increased. The total number of experimental points used to construct the final RF is 2n+1, thus the quadratic polynomials without cross terms is used as the RF, as follows

$$\bar{G}(\mathbf{X})=a+\sum_{i=1}^{n}b_ix_i+\sum_{i=1}^{n}c_ix_i^2 \tag{14}$$

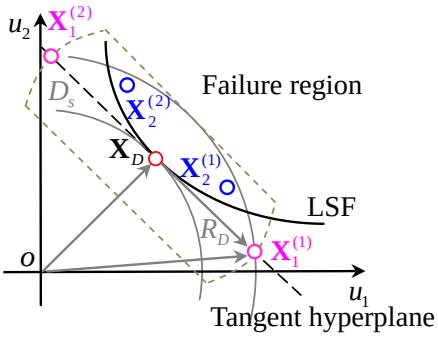

Fig. 7 Experimental points of the proposed method

where a , b_i and c_i are unknown coefficients.

3.3 Evaluation of failure probability

In the paper, the MCS is performed to evaluate the failure probability by using the RF. The failure probability is given by

$$P_f = \frac{m_1}{N_s} \tag{15}$$

where N_s is the total number of sample points for MCS, m_1 is the total number of failure points in the whole design space.

As seen from Section 2, the region outside of the sub-region of interest has small contribution to failure probability, and the contribution to failure probability coming from the sub-region of interest should be equal to 1-ε_p. For a given value of ε_p, such as 0.05, the size of sub-region of interest can ensure that the failure probability obtained by using the RF is satisfactory. Thus, in the paper, the RF only in the sub-region of interest is utilized to evaluate the failure probability. Eq. (15) can be rewritten as follows

$$P_f = \frac{P_{f,D_s}}{1-\varepsilon_p} = \frac{m_2}{(1-\varepsilon_p)N_s} \tag{16}$$

where P_{f,D_s} is the failure probability coming from the sub-region of interest, m_2 is the total number of failure points in the sub-region of interest.

3.4 Discussion on efficiency and accuracy

Since the proposed method is constructed based on the design point resulting from FORM, the efficiency of the proposed method is slightly lower than that of FORM. As seen from experimental design of the proposed method, the number of LSF evaluations of the proposed method is m_3+2n, where m_3 is the number of LSF evaluations to obtain the design point by using FORM, n is the number of random variables.

Since the quadratic polynomials RF is used in the proposed method, the accuracy of proposed

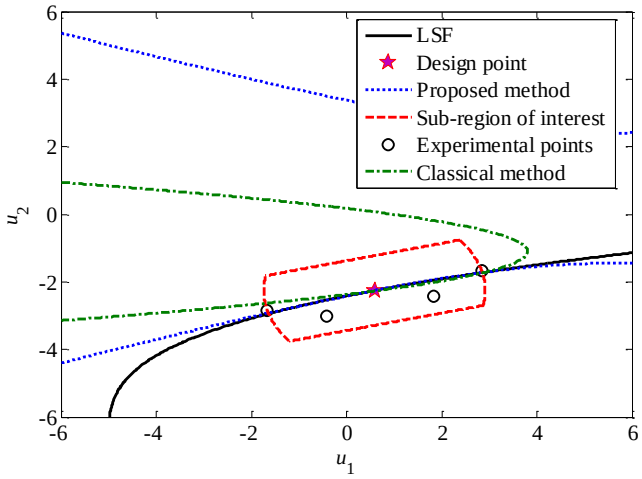

Fig. 8 Example 1: response surface approximations (ε_p=0.05)

method should be higher than that of FORM. In addition, the proposed method has a distinct advantage compared with the classical RSM in terms of the evaluation of failure probability. The advantages of the proposed method will be shown in examples.

3.5 Discussion on parameter

In the paper, the importance level ε_p is introduced. Following the definition of the sub-region of interest, if the value of ε_p tends to 0, the size of sub-region of interest will tend to infinity. If the value of ε_p tends to 1, the size of sub-region of interest will tend to 0. The parameter ε_p characterizes the size of sub-region of interest: lower it is, bigger is the sub-region of interest. As seen from Eq. (2), the value of ε_p should be relatively low, such as 0.05 or 0.1. Actually, the parameter ε_p defines the sub-region of interest outside of which the failure probability is considered as negligible.

4. Numerical examples

In the paper, the importance sampling MCS is performed to assess the accuracy of failure probability obtained by using the RF. Then 10^6 simulations are performed by using the LSF and the RF respectively. From this comparison it is possible to understand if the RF is close to the actual LSF. The failure probability obtained by using FORM is given by $P_f=\Phi(-\beta)$. A parametric analysis is performed with respect to the parameter ε_p, the different values (0.05 and 0.1) are considered.

4.1 Example 1: a cantilever beam

The structure is a cantilever beam with a rectangular cross-section and is subjected to a uniformly distributed load (Allaix and Carbone 2011). The LSF is given by

$$G(\mathbf{X}) = 18.46154 - 7.476923 \times 10^{10} \frac{x_1}{x_2^3} \tag{17}$$

where x_1 and x_2 are realizations of the random variables $X_1 \sim N(0.001, 0.002)$ and $X_2 \sim N(250, 37.5)$.

In the standard normal space (**U** space), the results obtained by using the proposed method and classical RSM are shown graphically in Fig. 8. As seen from Fig. 8, the RFs of proposed method and classical RSM both deviate from the actual LSF in the region outside of the sub-region of interest. The main reason can be explained as follows: the proposed method and classical RSM are both utilize a quadratic polynomial function without cross terms to approximate the actual LSF. Actually, it is very difficult that a quadratic polynomial function has good global fitting precision to the actual LSF, especially for implicit nonlinear LSFs. However, in the structural reliability analysis, the main region influencing failure probability is the local region around the design point, namely the sub-region of interest. Thus, the RF only need approximate the actual LSF better in the sub-region of interest where it is evaluated. As seen from Fig. 8, the proposed method can lead to a better approximation of the actual LSF in the sub-region of interest.

The numerical results are listed in Table 1. NFE in Table 1 denotes the number of LSF evaluations, which may be understood as a measure of efficiency. As seen from the results in Table 1, the accuracy of the proposed method is satisfactory in terms of the failure probability, and the efficiency of the proposed method is also satisfactory compared with the ones of other methods. Moreover, the failure probability obtained by using the proposed method does not show any significant dependence on the parameter ε_p.

As seen from the results in Table 1, the failure probability obtained by using the classical RSM is extremely inaccurate. The main reason can be explained as follows: the RF obtained by the classical RSM deviates from the actual LSF in the region outside of the sub-region of interest, if the MCS is performed to evaluate the failure probability by using classical RSM, a large number of unreasonable failure points will be given, the results are shown in Fig. 9. As seen from Fig. 9, since the RF obtained by the classical RSM deviates from the actual LSF in the top half of Fig. 9, a large number of unreasonable failure points (red points in Fig. 9) are given. Actually, it is very difficult to obtain good global fitting precision when a quadratic polynomial function is utilized to replace the actual LSF. Whereas it is relatively easy to obtain good local fitting precision in the

Table 1 Example 1-Comparison of analysis results

Method	u_1^*	u_2^*	β	NFE	P_f
Rajashekhar and Ellingwood (1993)	0.395	-2.306	2.3395	25	9.54×10^{-3}
Gayton *et al.* (2003)	0.586	-2.243	2.318	24	Not avail.
Duprat and Sellier (2006)	0.595	-2.253	2.3302	19	Not avail.
Allaix and Carbone (2011)	0.595	-2.258	2.33	50	9.75×10^{-3}
Elegbede (2005)	0.595	-2.253	2.3309	69300	9.88×10^{-3}
FORM	0.588	-2.256	2.3309	30	9.88×10^{-3}
Classical RSM	0.409	-2.304	2.3386	48	4.27×10^{-1}
Proposed RSM (ε_p=0.1)	0.588	-2.256	2.3309	34	9.78×10^{-3}
Proposed RSM (ε_p=0.05)	0.588	-2.256	2.3309	34	9.75×10^{-3}
MCS	-	-	-	10^6	9.79×10^{-3}

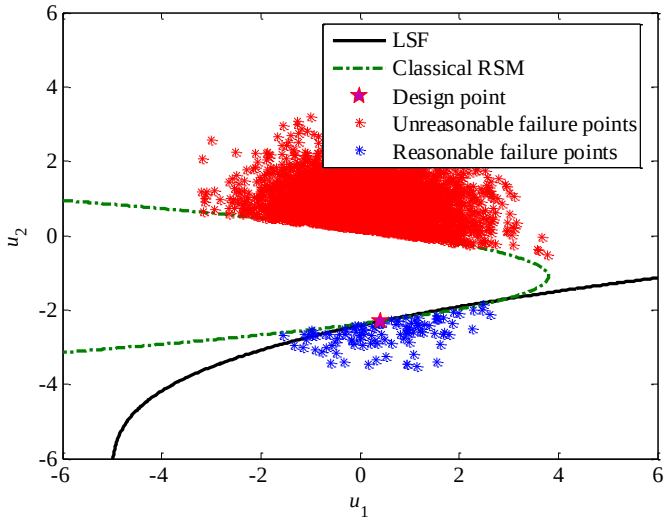

Fig. 9 Example 1: failure points obtained by using the classical RSM

sub-region of interest. In the paper, the proposed sub-region of interest is the local region around the design point, the RF only in the sub-region of interest is utilized to evaluate the failure probability resulting in satisfactory results. Thus, the proposed method has a distinct advantage compared with the classical RSM in terms of the evaluation of failure probability.

As seen from the results in Table 1, the failure probability given by Rajashekhar and Ellingwood (1993) is very close to the one obtained by using MCS. However, the random variables were limited to a special region in the studies of Rajashekhar and Ellingwood (1993). In general, figures can't be obtained for a problem of high dimension, so that bounds of random variables can't be obtained based on results of figures. Thus, it is necessary to define the size of main region influencing failure probability, namely the sub-region of interest must be defined clearly.

4.2 Example 2: a quadratic LSF with a cross term

A quadratic LSF with a cross term is considered, as follows

$$G(\mathbf{X}) = 0.1(u_1 - u_2)^2 - \frac{(u_1 + u_2)}{\sqrt{2}} + 2.5 \tag{18}$$

where u_1 and u_2 are realizations of standard normal variables.

Since the proposed method and the classical RSM both do not contain cross terms, the example is used to show the influence of cross terms on two methods. The results obtained by using the proposed method and classical RSM are shown graphically in Fig. 10. As seen from Fig. 10, the proposed method can obtain a better approximation of the LSF in the sub-region of interest.

The numerical results are listed in Table 2. As seen from the results in Table 2, the proposed method is better than the classical method, and does not show any significant dependence on the parameter ε_p. The accuracy of the proposed technique by Allaix and Carbone (2011) is the best in

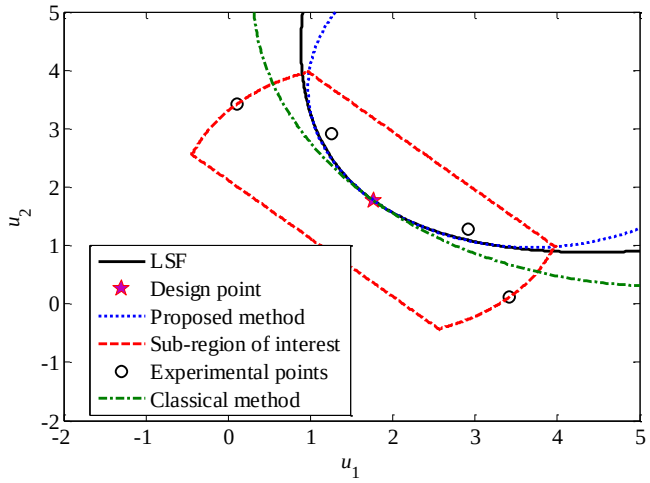

Fig. 10 Example 2: Response surface approximations (ε_p=0.05)

Table 2 Example 2-Comparison of analysis results

Method	u_1^*	u_2^*	β	NFE	P_f
Allaix and Carbone (2011)	1.761	1.761	2.4904	25	4.30×10^{-3}
Borri and Speranzini (1997)	1.768	1.768	2.4996	Not avail.	Not avail.
FORM	1.768	1.767	2.5000	10	6.21×10^{-3}
Classical RSM	1.768	1.768	2.5000	18	5.02×10^{-3}
Proposed RSM (ε_p=0.1)	1.768	1.767	2.5000	14	4.13×10^{-3}
Proposed RSM (ε_p=0.05)	1.768	1.767	2.5000	14	4.14×10^{-3}
MCS	-	-	-	10^6	4.25×10^{-3}

terms of the failure probability. However, the results obtained by using the proposed method are acceptable in terms of its accuracy and efficiency. The accuracy and the efficiency of the proposed method are both better than those of the classical RSM. The accuracy of the proposed method is obviously better than that of FORM with increase in small computational efforts.

4.3 Example 3: a frame structure

A three-bay five-storey rigid frame structure is considered as illustrated in Fig. 11. It was studied in several papers (Roussouly *et al.* 2013, Blatman and Sudret 2010). There are 21 studied variables: 3 horizontal loads (form P_1 to P_3), 8 moments of inertia (from I_1 to I_8), 8 cross-section areas (from A_1 to A_8) and 2 Young's moduli (E_1 and E_2). These properties, associated to beam elements, are listed in Table 3. Distributions, mean values and standard deviations of random variables are given in Table 4. Here, some variables are assumed to be correlated:

1. Cross-section areas and moments of inertia of the same element with a coefficient ρ_{A_i,I_i} =0.95;

2. All others geometrical properties with coefficients $\rho_{A_iA_j} = \rho_{I_iI_j} = \rho_{A_iI_j}$ =0.13;

3. The correlation of two Young's moduli is equal to ρ_{E_1,E_2} =0.9;
4. All remaining variables are assumed to be uncorrelated.

The structure is studied for reliability analysis with the following LSF

$$G(\mathbf{X}) = 0.06 - \Delta(\mathbf{X}) \tag{19}$$

where Δ is the horizontal displacement on the top-right corner of the structure.

In the studies of Roussouly *et al.* (2013) and Blatman and Sudret (2010), the reference failure probability P_f^{REF} is given by the importance sampling MCS, the corresponding generalized reliability index is given by $\beta^{REF} = -\Phi^{-1}(P_f^{REF})$. Thus, the failure probabilities in the studies of Roussouly *et al.* (2013), Blatman and Sudret (2010) can be calculated by $P_f=\Phi(-\beta^{REF})$.

The numerical results are reported in Table 5. As seen from the results in Table 5, the failure probability obtained by using FORM is most inaccurate, thus the nonlinear of LSF should be high. The failure probability obtained by using the proposed method is close to the one obtained by using MSC, and does not show any significant dependence on the parameter ε_p. The accuracy and the efficiency of the proposed method are both better than those of the classical RSM. The accuracy of the proposed method is obviously better than that of FORM as a result of utilizing the sub-region of interest. The example shows that the proposed method using the sub-region of interest is reasonable and feasible for a engineering structure with a large number of correlated random variables.

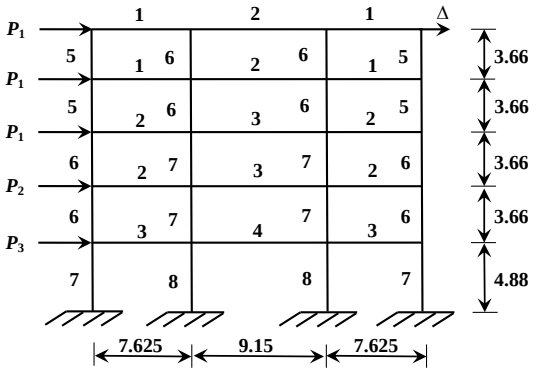

Fig. 11 Example 3: a frame structure (unit, m)

Table 3 Example 3: frame element properties

Element	Modulus of elasticity	Moment of inertia	Cross section
1	E_1	I_5	A_5
2	E_1	I_6	A_6
3	E_1	I_7	A_7
4	E_1	I_8	A_8
5	E_2	I_1	A_1
6	E_2	I_2	A_2
7	E_2	I_3	A_3
8	E_2	I_4	A_4

Table 4 Example 3: statistical parameters and distributions of the random variables

Variable	Distribution	Unit	Mean value	Standard deviation
P_1	Lognormal	kN	133.454	40.04
P_2	Lognormal	kN	88.97	35.59
P_3	Lognormal	kN	71.175	28.47
E_1	Normal	kN/m^2	2.1738×10^{7}	1.9152×10^{6}
E_2	Normal	kN/m^2	2.3796×10^{7}	1.9152×10^{6}
I_1	Normal	m^4	8.1344×10^{-3}	1.0834×10^{-3}
I_2	Normal	m^4	1.1509×10^{-2}	1.2980×10^{-3}
I_3	Normal	m^4	2.1375×10^{-2}	2.5961×10^{-3}
I_4	Normal	m^4	2.5961×10^{-2}	3.0288×10^{-3}
I_5	Normal	m^4	1.0812×10^{-2}	2.5961×10^{-3}
I_6	Normal	m^4	1.4105×10^{-2}	3.4615×10^{-3}
I_7	Normal	m^4	2.3279×10^{-2}	5.6249×10^{-3}
I_8	Normal	m^4	2.5961×10^{-2}	6.4902×10^{-3}
A_1	Normal	m^2	3.1256×10^{-1}	5.5815×10^{-2}
A_2	Normal	m^2	3.7210×10^{-1}	7.4420×10^{-2}
A_3	Normal	m^2	5.0606×10^{-1}	9.3025×10^{-2}
A_4	Normal	m^2	5.5815×10^{-1}	1.1163×10^{-1}
A_5	Normal	m^2	2.5302×10^{-1}	9.3025×10^{-2}
A_6	Normal	m^2	2.9117×10^{-1}	1.0232×10^{-1}
A_7	Normal	m^2	3.7303×10^{-1}	1.2093×10^{-1}
A_8	Normal	m^2	4.1860×10^{-1}	1.9537×10^{-1}

Table 5 Example 3: comparison of analysis results

Method	β	NFE	P_f
Full PCE (Blatman and Sudret 2010)	Not avail.	3724	1.59×10^{-4}
Sparse PCE (Blatman and Sudret 2010)	Not avail.	450	1.53×10^{-4}
Roussouly *et al.* (2013)	Not avail.	149	1.42×10^{-4}
FORM	3.7836	110	7.73×10^{-5}
Classical RSM	3.7838	264	1.88×10^{-4}
Proposed RSM (ε_p=0.1)	3.7838	194	2.17×10^{-4}
Proposed RSM (ε_p=0.05)	3.7838	194	2.18×10^{-4}
MCS	-	10^6	2.24×10^{-4}

5. Conclusions

In this study, the concept of sub-region of interest is constructed. The sub-region of interest can clearly define the size of main region influencing failure probability. An improved RSM is proposed based on the sub-region of interest. The efficiency of the proposed method is slightly lower than that of FORM. However, since the experimental points of proposed method can

consider the size of main region influencing failure probability, the accuracy of the proposed method is better than that of FORM in terms of the evaluation of failure probability.

Numerical examples show that the efficiency and the accuracy of proposed method are both satisfactory in terms of the number of LSF evaluations. Moreover, the failure probability obtained by using the proposed method does not show any significant dependence on the parameter ε_p. The parameter ε_p characterizes the size of sub-region of interest: lower it is, bigger is the sub-region of interest. Actually, the parameter ε_p defines the sub-region of interest outside of which the failure probability is considered as negligible. Thus, $\varepsilon_p \in [0.05, 0.1]$ is recommended for possible users. Through these examples, it can be seen that the proposed method and the sub-region of interest are reasonable and feasible.

Since the concept of sub-region of interest is constructed based on the design point obtained by using FORM, the proposed method may be not suitable for approximating a LSF with multiple design points. Further investigation of the proposed method should be required without increase in computational efforts. However, the concept of sub-region of interest is clear, it can provide the theoretical basis for utilization of RSMs in assessing engineering structural safety.

Acknowledgements

The research described in the paper was financially supported by the Aerospace Science Foundation of China (Grant No.2013ZA54004) and the General Projects for Liaoning in University of China (Grant No.L2014072).

References

Allaix, D.L. and Carbone, V.I. (2011), "An improvement of the response surface method", *Struct. Saf.*, **33**(2), 165-172.

Basaga, H.B., Bayraktar, A. and Kaymaz, I. (2012), "An improved response surface method for reliability analysis of structures", *Struct. Eng. Mech.*, **42**(2), 175-189.

Blatman, G. and Sudret, B. (2010), "An adaptive algorithm to build up sparse polynomial chaos expansions for stochastic finite element analysis", *Prob. Eng. Mech.*, **25**(2), 183-97.

Borri, A. and Speranzini, E. (1997), "Structural reliability analysis using a standard deterministic finite element code", *Struct. Saf.*, **19**(4), 361-382.

Bucher, C.G. and Bourgund, U. (1990), "A fast and efficient response surface approach for structural reliability problems", *Struct. Saf.*, **7**(1), 57-66.

Ditlevsen, O. and Madsen, H.O. (1996), *Structural Reliability Methods*, Chischester,Wiley, UK.

Duprat, F. and Sellier, A. (2006), "Probabilistic approach to corrosion risk due to carbonation via an adaptive response surface method", *Prob. Eng. Mech.*, **21**(3), 207-216.

Elegbede, C. (2005), "Structural reliability assessment based on particles swarm optimization", *Struct. Saf.*, **27**(2), 171-186.

Gavin, H.P. and Yau, S.C. (2008), "High-order limit state functions in the response surface method for structural reliability analysis", *Struc. Saf.*, **30**(2), 162-179.

Gayton, N., Bourinet, J.M. and Lemaire, M. (2003), "CQ2RS: a new statistical approach to the response surface method for reliability analysis", *Struct. Saf.*, **25**(1), 99-121.

Hasofer, A.M. and Lind, N.C. (1974), "Exact and invariant second-moment code format", *J. Eng. Mech.*, ASCE, **100**(1), 111-121.

Kaymaz, I. and Chris, A.M. (2005), "A response surface method based on weighted regression for structural

reliability analysis", *Prob. Eng. Mech.*, **20**(1), 11-17.
Khuri, A.I. and Cornell, J.A. (1997), *Response Surfaces: Design and Analyses*, Marcel and Dekker, New York.
Kim, S. and Na, S. (1997), "Response surface method using vector projected sampling points", *Struct. Saf.*, **19**(1), 3-19.
Kiureghian, D.A., Lin, H.Z. and Hwang, S.J. (1987), "Second order reliability approximations", *J. Eng. Mech.*, ASCE, **113**(8), 1208-1225.
Mohammadi, R., Massumi, A and Meshkat-Dini, A. (2015), "Structural reliability index versus behavior factor in RC frames with equal lateral resistance", *Earthq. Struct.*, **8**(5), 995-1016.
Myers, R.H. and Montgomery, D.C. (1995), *Response Surface Methodology: Process and Product Optimization using Designed Experiments*, Wiley, Chischester, UK.
Nguyen, X.S., Sellier, A., Duprat, F. and Pons, G. (2009), "Adaptive response surface method based on a double weighted regression technique", *Prob. Eng. Mech.*, **24**(2), 135-143.
Rackwitz, R. and Fiessler, B. (1978), "Structural reliability under combined random load sequences", *Comput. Struct.*, **9**(5), 489-494.
Rajashekhar, M.R. and Ellingwood, B.R. (1993), "A new look at the response surface approach for reliability analysis", *Struct. Saf.*, **12**(3), 205-220.
Roussouly, N., Petitjean, F. and Salaun, M. (2013), "A new adaptive response surface method for reliability analysis", *Prob. Eng. Mech.*, **32**,103-15.
Su, G., Jiang, J., Yu, B. and Xiao, Y. (2015), "A Gaussian process-based response surface method for structural reliability analysis", *Struct. Eng. Mech.*, **56**(4), 507-534.
Wong, S.M., Hobbs, R.E. and Onof, C. (2005), "An adaptive response surface method for reliability analysis of structures with multiple loading sequences", *Struct. Saf.*, **27**(4), 287-308.
Zhao, W. and Qiu, Z. (2013), "An efficient response surface method and its application to structural reliability and reliability-based optimization", *Finite Elem. Anal. Des.*, **67**, 34-42.
Zhao, W., Qiu, Z. and Yang, Y. (2013), "An efficient response surface method considering the nonlinear trend of the actual limit state", *Struct. Eng. Mech.*, **47**(1), 45-58.

CC